Eur. Phys. J. D **5**, 275–281 (1999)

THE EUROPEAN PHYSICAL JOURNAL D

EDP Sciences

Systematic studies on hydrogen cluster beam production

A. Khoukaz[a], T. Lister, C. Quentmeier, R. Santo, and C. Thomas

Institut für Kernphysik, Westfälische Wilhelms-Universität, 48149 Münster, Germany

Received: 17 July 1998 / Received in final form and Accepted: 16 October 1998

Abstract. We present systematic studies on the absolute density of hydrogen cluster beams produced by using Laval-nozzles. Measurements of the cluster beam density as function of the nozzle temperature and the gas input pressure result in maximum cluster beam densities for cases where the gas is already in a supersaturated state before passing the nozzle. The influence of the gas flow through the nozzle on the starting temperature of clustering and the temperature dependence of the cluster beam density at constant gas flows are studied.

PACS. 36.40.-c Atomic and molecular clusters – 36.40.Qv Stability and fragmentation of clusters

1 Introduction

Atomic and molecular clusters are of growing interest in scientific research. Being in a state between the microscopic and macroscopic "world" they offer useful properties for several applications: for fusion devices cluster sources can be used for fuel injection [1,2], and in the case of gas-surface interaction cluster sources allow to study conditions relevant for low altitude satellites [3]. Furthermore, cluster beams are of growing interest for accelerator experiments. Produced in Laval-nozzles, they can be used as windowless targets of very high purity. The absolute density can easily be varied over orders of magnitude by changing the nozzle temperature or the gas input pressure. Different to gas-jet beams they provide a spatially well-defined target beam with a homogeneous density distribution. In practice, the knowledge of sensitive parameters like the nozzle diameter or the nozzle temperature concerning the cluster beam density are essential for an optimized cluster target. Since the processes of cluster formation are up to now only poorly understood, we have performed a number of detailed investigations on hydrogen cluster beams. The similarity of the installation (described in Sect. 2) to the cluster targets for the COSY11 [4] and ANKE [5] experiments enables to take advantage of the presented results.

2 Experimental

The measurements have been carried out at the Münster cluster target device shown in Figure 1. It consists of three main parts: the cluster source, the analyzing chamber and the beam dump. The clusters with a typical size of 10^3–10^4 atoms [6] are produced in a Laval-nozzle (Fig. 2)

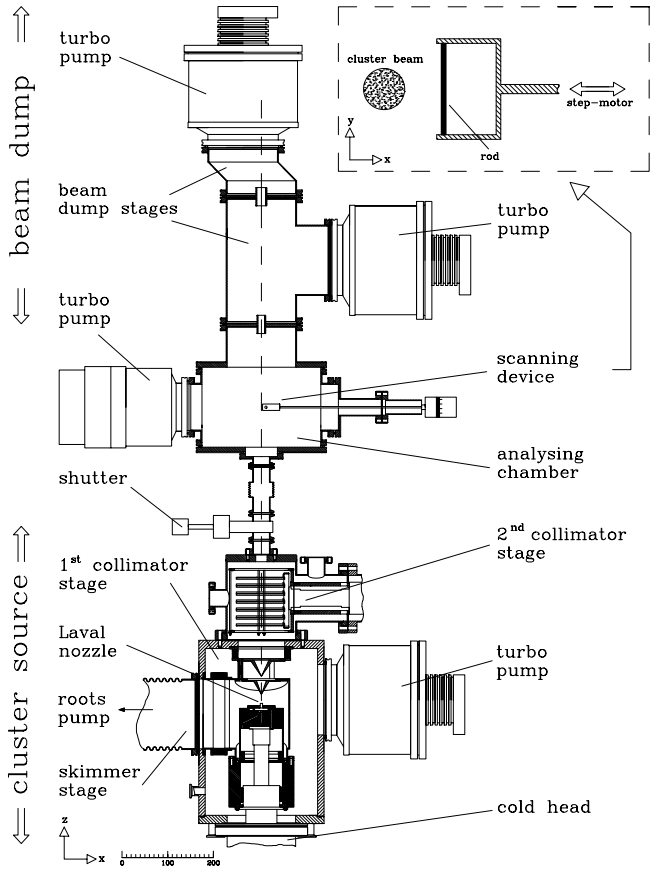

Fig. 1. Sketch of the cluster target installation.

mounted on top of a cold head which provides temperatures down to ∼ 20 K. To vary the temperature a heating system is connected to this assembly. At 20 mm behind the nozzle the produced cluster beam, surrounded by a gas

[a] e-mail: khoukaz@ikp.uni-muenster.de

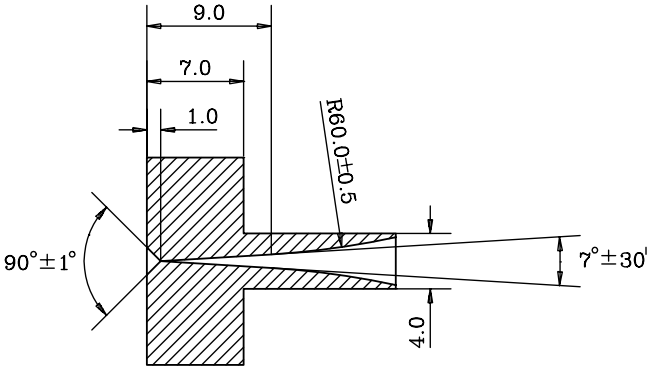

Fig. 2. Sketch of a Laval-nozzle.

beam, hits a conical aperture with an opening of 700 μm, acting as a skimmer. As consequence, only a well-prepared part of the cluster beam passes this vacuum stage and nearly the whole gas beam remains in the skimmer stage and is pumped by a roots pump. Between the following first and second collimator stage another conical aperture with a diameter of 900 μm is placed in order to define the cluster beam diameter and to hold back residual gas. After this stage a cluster beam with a constant angular divergence is available, passes the next differential pumping stage (second collimator stage) and enters the analyzing chamber. For more details see [4].

The analyzing chamber is equipped with a step-motor controlled device to scan the passing cluster beam in a plane perpendicular to its spread direction (Fig. 1). The scanning rod with a thickness of 1.0 mm can be positioned in units of 1/24 mm. If the rod is placed inside the cluster beam, a part of the beam is stopped and converted into a gas load which can be recorded by an ionization vacuummeter. Thus, this system is sensitive to the absolute cluster beam density and to the overlap between the rod and the cluster beam and can be used to obtain information about the size and the position of the beam. Furthermore, if the rod is placed at a fixed position inside the cluster beam, this system allows to monitor the density of the cluster beam. After this stage the beam enters the beam dump, where the clusters are destroyed and form an appreciable gas load. Although a large fraction of this can directly be pumped by the turbo pump, a non-negligible amount remains in this chamber and affects the vacuum in the analyzing chamber. To minimize this effect the beam dump consists of differentially pumped vacuum chambers which are separated by small apertures. The diameters of these apertures (15 mm and 20 mm) are as small as possible but big enough to allow an undisturbed passage of the cluster beam.

2.1 Profiles

In Figure 3 a density profile of a hydrogen cluster beam is shown. This profile was measured 0.65 m behind the nozzle with the scanning system described above. The cluster beam was scanned in steps of 1/8 mm and the resulting pressure in the analyzing chamber was measured. If

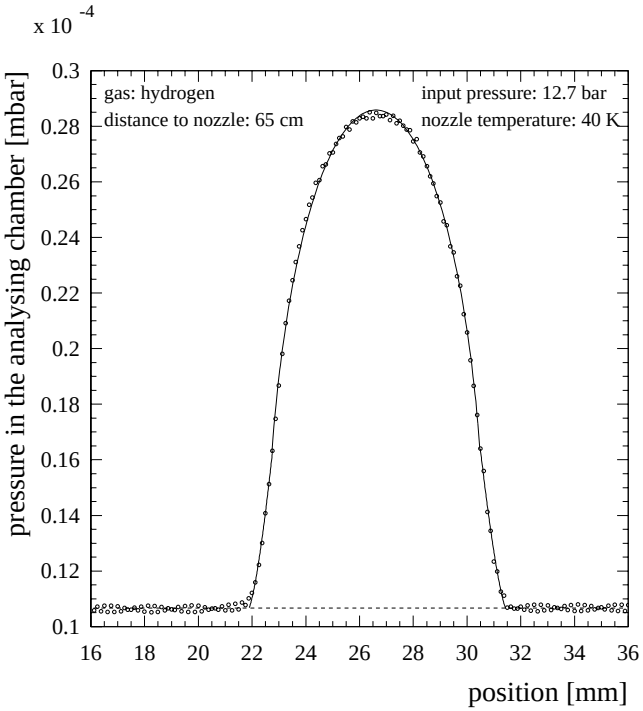

Fig. 3. Profile of a cluster beam measured with the scanning device. The fit (solid line) is based on the assumption of a homogeneous cylindrical cluster beam.

the volume density distribution is homogeneous the pressure will be proportional to the overlap between the cluster beam and the rod and can be described by a circle function. The shown calculation (solid line), assuming a homogeneous cylindrical cluster beam with a diameter of 8.5 mm, fits very well with the measured curve. In contrast to this steep rise, a molecular gas-jet beam has a Gaussian profile. This fact is of great interest for accelerator experiments where the knowledge of the interaction point is important for the reconstruction of outgoing tracks.

The stopping of a certain part of the cluster beam in the analyzing chamber by the rod causes an increase of the vacuum pressure. This increase corresponds to a gas flow G, which can be calculated if the pumping speed in this chamber is known. In combination with the cluster beam diameter, the rod diameter and the cluster beam velocity this value allows to calculate the absolute cluster beam density. Except for the cluster velocity all of these parameters can usually be determined. Up to now there exist no measurements of the velocity of hydrogen clusters relevant to our working conditions. Therefore, we calculate the velocity of the gas beam after having passed the nozzle and assume that the produced cluster beam has the same velocity. Calculations of the maximum gas beam velocity u_{max} can be found in [7] and result in

$$u_{max} = \sqrt{\frac{2\kappa}{\kappa - 1}\frac{kT_0}{m}} \tag{1}$$

with $\kappa = c_p/c_v$, k the Boltzmann constant, T_0 the temperature of the gas before passing the nozzle and m as the

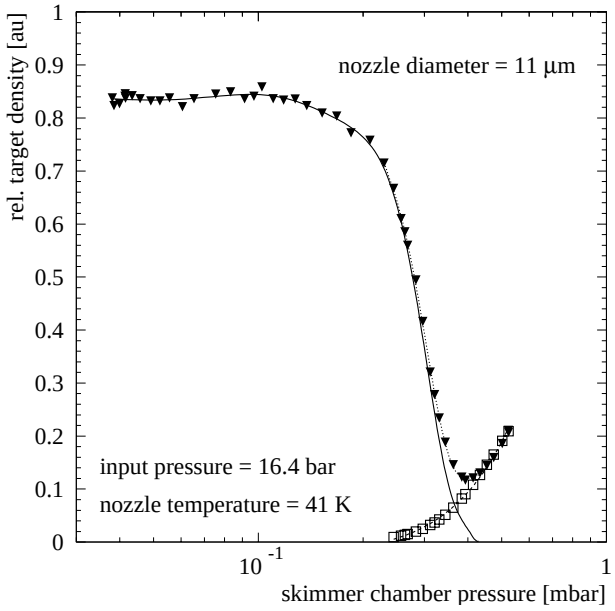

Fig. 4. Stability of hydrogen clusters as function of the residual gas pressure.

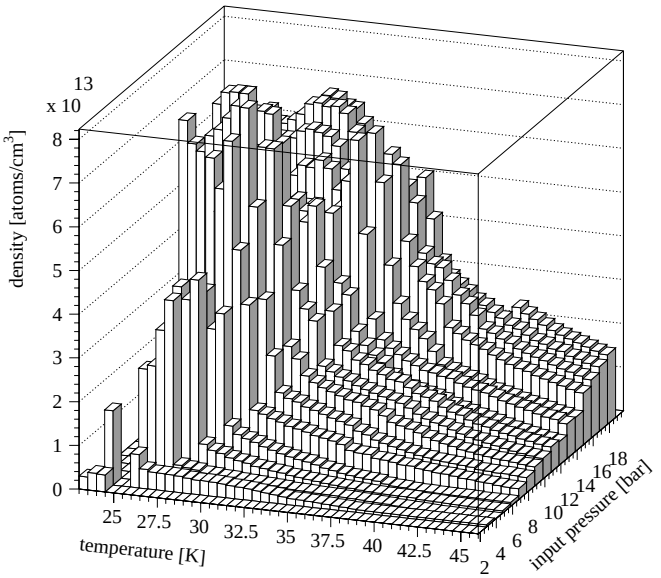

Fig. 5. Cluster beam density in the analyzing chamber as function of the nozzle temperature and the gas input pressure. This measurement was done 65 cm behind the nozzle using a 11 μm nozzle.

mass of the gas per mol. These calculations are based on the assumption that the total inner energy is completely converted into kinetic energy. By this procedure it is possible to extract absolute cluster beam densities from the described measurements.

2.2 Cluster stability

For an optimized production of cluster beams and studies of the cluster beam density as function of operation parameters it is essential to avoid conditions which lead to the destruction of the cluster beam. Systematic measurements showed that hydrogen cluster beams are stable and can travel over several meters through vacuum chambers as long as high vacuum conditions are fulfilled. At vacuum pressures above 10^{-1} mbar the destruction of clusters due to scattering with residual gas can not be neglected. For a detailed investigation a stable hydrogen cluster beam was produced and the movable rod was placed in the center of the cluster beam. Additionally to the previous described target installation, a needle valve was connected to the skimmer chamber in order to externally adjust the hydrogen gas load. This gas load adds to the one resulting from the constant gas flow through the nozzle. The lowest skimmer chamber pressure results, of course, at closed valve. During the following measurement the pressure in that chamber was increased by opening the valve. In Figure 4 the resulting cluster beam density in the analyzing chamber as function of the skimmer chamber pressure is shown (triangle symbols). Additionally, a background measurement was performed without a cluster beam (open squares) which shows an apparent increase of the cluster beam density only above $\sim 3 \times 10^{-1}$ mbar due to the residual gas load from the skimmer chamber. To obtain the real cluster beam density the background measurement (dashed line) was subtracted from the previous data (dotted line) resulting in the solid line. It can be seen that at pressures below 10^{-1} mbar the cluster beam density is constant. Above this value the cluster beam density decreases rapidly and at a pressure of $\sim 4 \times 10^{-1}$ mbar approaches zero.

This result shows that for the design of a cluster source and its operation it is very important to have sufficient pumping capacities, especially in the skimmer stage. On the other hand no UHV conditions are needed in order to achieve highest cluster beam densities.

2.3 Hydrogen cluster beam density

For the operation of a cluster beam facility it is essential to know how to adjust the cluster beam density. An easy and effective method is to change the temperature of the nozzle or to vary the gas input pressure. To get detailed information about the influence of the nozzle temperature T and the gas input pressure p on the cluster beam density ρ in the analyzing chamber, we determined $\rho(p,T)$ in a temperature range of $T \sim 25$–46 K at operation pressures of $p \sim 2$–18 bar [11]. The result can be seen in Figure 5. As expected, the lowest density $\rho(p,T)$ shows up at highest temperatures and lowest pressures. Starting at high temperatures and fixing the pressure, the density increases slowly with decreasing temperature. At a certain temperature the density suddenly increases strongly and reaches maximum values in the low temperature region. A top view of this figure with the vapour pressure curve for hydrogen included is shown in Figure 6. It is clearly seen that the described strongest increase of ρ is located at (p,T)-pairs lying on the vapour pressure curve. Highest

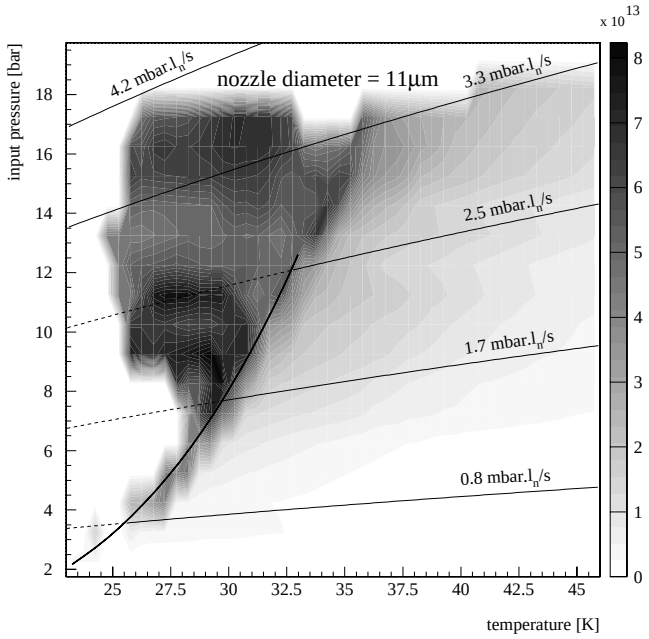

Fig. 6. Cluster beam density in [atoms/cm^3] as function of the nozzle temperature and the gas input pressure. The solid line corresponds to the vapour pressure curve of hydrogen. Also shown are (p,T)-pairs with constant gas flows through the nozzle.

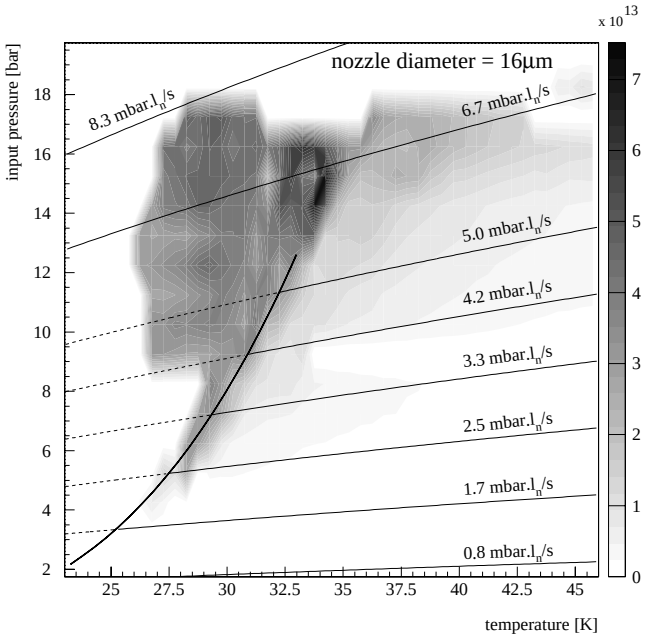

Fig. 7. Cluster beam density in [atoms/cm^3] as function of the nozzle temperature and the gas input pressure using a 16 μm nozzle.

densities ρ are achieved in a mode where the gas is already in a supersaturated state before passing the nozzle. Furthermore, (p,T)-pairs with the same gas flow through the nozzle are plotted (solid/dashed lines). These "cooling curves" show that for reaching highest densities it is not necessary to operate the device at highest gas flows. In Figure 7 the same measurement is shown but for a nozzle with a diameter of 16 μm. Again, highest densities are achieved by operating the device with supersaturated gas in front of the nozzle. Comparing both measurements it is obvious that at the same (p,T)-pair the smaller nozzle yields higher densities ρ and that for reaching the same density only half of the gas flow is needed compared to the bigger nozzle (16 μm). These results are very important for design and operation of a cluster beam device. First of all, it is possible to derive values of parameters (nozzle diameter, nozzle pressure and temperature) from these "density maps" which are necessary to reach a certain density. Furthermore, these measurements show how to adjust the density during a cluster beam operation.

Usually cluster targets are operated with gas being in the "normal" gas phase in front of the nozzle [8–10]. Different to this our cluster target for the COSY11 experiment at the FZ Jülich [4] takes advantage of the described effect that highest densities can be reached by feeding the nozzle with supersaturated gas.

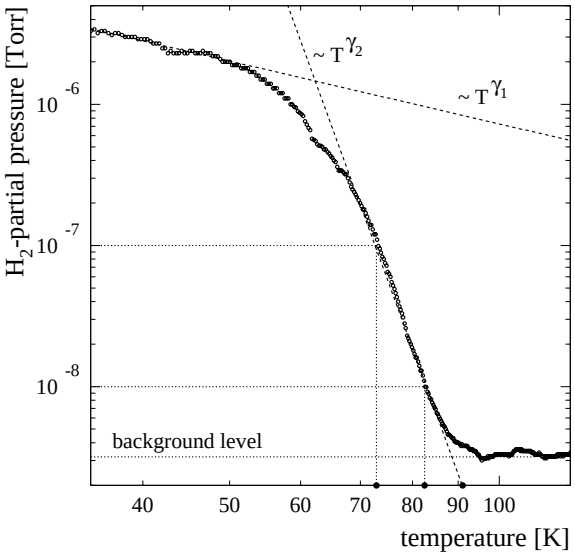

Fig. 8. Cooling curve for hydrogen, measured 65 cm behind the nozzle (11 μm) with a constant gas flow of 3.3 mbar l_n/s.

2.4 Cooling curves

Valuable information about the starting point of cluster formation and the cluster beam density as function of parameters like the nozzle temperature can be derived from measuring cooling curves: the partial pressure of the clustered gas in the analyzing chamber is recorded at fixed gas flows through the nozzle as function of the nozzle temperature. As described above, the background subtracted partial pressure is proportional to the cluster beam density.

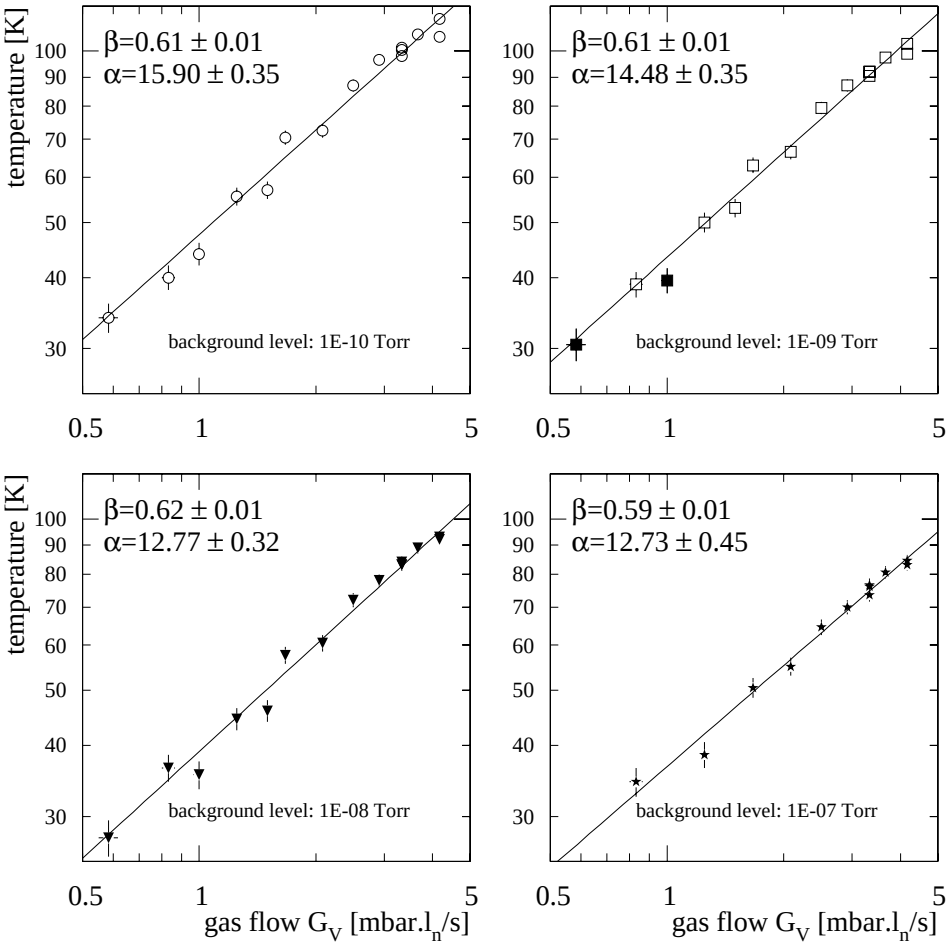

Fig. 9. Starting temperatures of clustering as function of the gas flow through the nozzle (16 μm), assuming gas background levels of 10^{-7}, 10^{-8}, 10^{-9} and 10^{-10} torr. The data were fitted with the function $T = \alpha {G_V}^{\beta}$. The data points indicated with solid symbols were directly extracted from the cooling curves while points indicated with open symbols were extracted by interpolating the high temperature part of the cooling curves.

In Figure 8 the result of such a measurement is plotted [12]. At high temperatures ($T > 95$ K) the partial pressure of hydrogen at a distance of 65 cm behind the nozzle is constant and corresponds to the actual background level in this pumping stage ($p_b \sim 3 \times 10^{-8}$ torr). At $T \leq 90$ K clustering becomes visible and the partial pressure increases over several orders of magnitude. Due to the hydrogen background level in this vacuum stage clustering becomes detectable only if the partial pressure caused by stopping the cluster beam is comparable to the background level. The "starting point" of clustering is therefore defined as the temperature $T(p_B)$ where clustering becomes visible in the presence of a certain background p_B.

As shown in Figure 8 the starting point $T(p_B)$ can be obtained by assuming a certain background level and extracting the corresponding temperature from the cooling curve (*e.g.* 10^{-7} torr / 72 K). For two special background levels (10^{-7} torr and 10^{-8} torr) this is indicated by dotted lines. To obtain more detailed information about the influence of the background level p_B and the gas flow G_V through the nozzle on the starting point, several cooling curves at different gas flows have been recorded using the

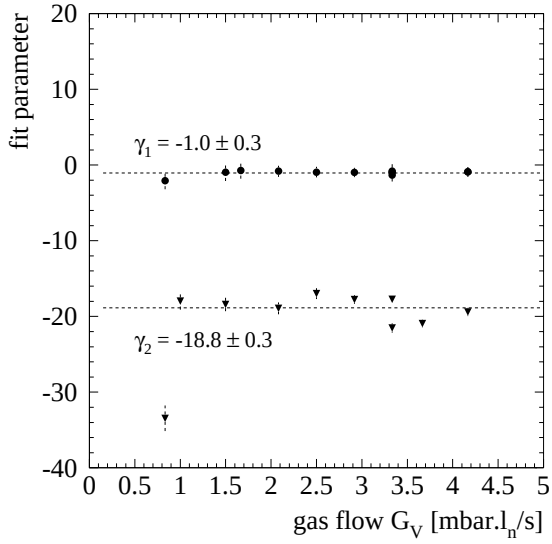

Fig. 10. Fit parameters γ_1 and γ_2 as function of the gas flow G_V, obtained from analyzing the described cooling curves.

Table 1. Values of the fit parameters ϵ_1 and γ_1 obtained from the low temperature part of cooling curves with given gas flow G_V.

gas flow [mbar l_n/s]	temp. region [K]	$\ln(\epsilon_1)$	γ_1
0.8	24.3–33.5	-8.04 ± 3.69	-2.06 ± 1.14
1.5	26.2–33.3	-12.59 ± 3.88	-0.97 ± 1.13
1.7	27.1–35.8	-11.38 ± 3.85	-0.72 ± 1.08
2.1	28.7–42.6	-11.82 ± 2.98	-0.83 ± 0.72
2.5	29.1–42.6	-10.15 ± 2.53	-0.94 ± 0.69
2.9	29.9–45.5	-9.88 ± 2.33	-0.98 ± 0.62
3.3	30.5–47.4	-10.19 ± 3.52	-0.80 ± 0.96
3.3	31.5–47.3	-9.65 ± 2.23	-0.95 ± 0.62
3.3	30.9–40.2	-7.98 ± 3.10	-1.31 ± 0.87
4.2	32.4–48.5	-9.55 ± 2.23	-0.93 ± 0.58
4.2	32.7–45.8	-9.83 ± 2.45	-0.88 ± 0.63

Table 2. Values of the fit parameters ϵ_2 and γ_2 obtained from the high temperature part of cooling curves with given gas flow G_V.

gas flow [mbar l_n/s]	temp. region [K]	$\ln(\epsilon_2)$	γ_2
0.8	33.4–35.6	102.21 ± 5.98	-33.45 ± 1.68
1.0	31.1–38.8	45.41 ± 4.09	-17.97 ± 1.15
1.5	40.9–48.7	51.94 ± 3.37	-18.43 ± 0.89
2.1	57.6–64.4	59.19 ± 3.23	-18.92 ± 0.79
2.5	67.2–74.4	54.25 ± 2.99	-16.99 ± 0.70
2.9	70.1–80.1	59.15 ± 2.47	-17.78 ± 0.57
3.3	76.9–84.7	76.98 ± 2.67	-21.54 ± 0.61
3.3	68.1–85.2	59.90 ± 1.92	-17.72 ± 0.44
3.7	78.2–89.5	75.64 ± 2.31	-20.93 ± 0.52
4.2	82.3–92.7	69.53 ± 2.44	-19.41 ± 0.55

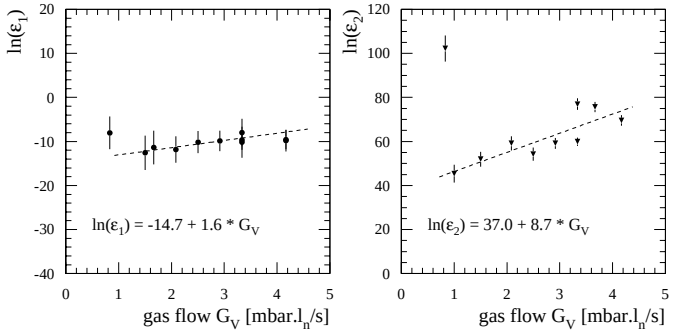

Fig. 11. Fit parameters ϵ_1 and ϵ_2 as function of the gas flow G_V.

16 μm nozzle. To avoid misinterpretation due to condensation of hydrogen gas in the gas feeding system, the following data have been extracted only from parts of the cooling curves without supersaturated gas in front of the nozzle. The result of these measurements can be seen in Figure 9. In this four double-logarithmic plots the starting temperature of clustering is shown as function of the gas flow through the nozzle. The four pictures correspond to background levels of 10^{-7}, 10^{-8}, 10^{-9} and 10^{-10} torr. The data points indicated by solid symbols were directly extracted from the cooling curves while points with open symbols were extracted by interpolating the high temperature part of the cooling curves. The data can well be described by a power fit function $T = \alpha\, {G_V}^{\beta}$ (solid lines). A comparison of the $\beta(p_B)$ values leads to the result that even if the background level differs by several orders of magnitude the slope β is constant within the error bars and results in a mean value of $\beta = 0.61 \pm 0.01$. With the knowledge of this parameter β and one pair (G_V^0, T^0) it is possible to predict, at a given background level p_B, starting temperatures T^i of clustering at gas flows G_V^i.

A further analysis of the cooling curves allows to describe the low and the high temperature part of the cooling curves by power fits of the form $\rho \sim p_{H_2} = \epsilon_i T^{\gamma_i}$ with ϵ_1 and γ_1 as the low temperature fit parameters and ϵ_2 and γ_2 as the high temperature fit parameters, respectively. In Figure 8 the fit curves are presented by dashed lines. The parameters ϵ_i and γ_i have been extracted from all measured cooling curves. In Figure 10 the individual slopes γ_i are presented as function of the gas flow G_V through the nozzle. It is seen that in good approximation both parameters are constant. The mean values of the parameters are found to be $\gamma_1 = -1.0 \pm 0.3$ and $\gamma_2 = -18.8 \pm 0.3$. This shows that the cluster beam density varies in both temperature regions according to $\rho \sim T^{\gamma_i}$ with universal scaling parameters γ_i independent of the gas flow G_V. The corresponding fit parameters ϵ_1 and ϵ_2 are shown in Figure 11. As expected from Figure 7 both parameters grow with increasing gas flow. Due to the fact that especially close to the starting point of clustering, the cluster beam density varies strongly with gas flow or nozzle temperature, the values of the ϵ parameters can easily differ by several orders of magnitude. The calculated parameters γ_i and ϵ_i are listed in Tables 1 and 2 for different gas flows. Furthermore, in both cases the temperature regions used for the fit calculation are displayed.

3 Summary

We have presented systematic studies on hydrogen cluster beam production using Laval-nozzles with diameters of 11 and 16 μm, respectively. For both nozzles two-dimensional maps of the cluster beam density as function of p and T have been recorded in the region of $T \sim$ 25–46 K and $p \sim$ 2–18 bar. It has been found that highest cluster beam densities can be achieved if the gas is already in a supersaturated state before passing the nozzle. Under this conditions the formation of hydrogen polymers in the gas reservoir is conceivable. While normally clustering starts

inside the nozzle, these polymers can enter the nozzle as initial stage of clustering and therefore could lead to an increase of the cluster yield or even the cluster size. Comparing both measurements, the nozzle with the smaller diameter leads to higher cluster beam densities at the same gas flows or at the same operating point (p, T).

The starting temperature of clustering (Sect. 2.4) was found to be proportional to ${G_V}^{\beta}$ with G_V as the gas flow through the nozzle (16 μm). The slope parameter resulted in $\beta = 0.61 \pm 0.01$, independent of the gas background level.

Cooling curves using the larger nozzle (16 μm) have been recorded at several gas flows through the nozzle. It turned out that both the high and the low temperature part of these curves can be described by power functions $\rho = \epsilon_i \; T^{\gamma_i}|_{G_V}$ with slope parameters γ_i. These parameters γ_i were found to be constant, independent of the gas flow G_V. Therefore, the high temperature parts of different cooling curves, showing $\rho(T)|_{G_V}$ close to the starting temperatures of clustering in a double-logarithmic plot, are parallel with a relative distance on the temperature scale proportional to ${G_V}^{\beta}$.

The authors would like to thank H.-W. Ortjohann for his advice and support during the design of the target device and our mechanical workshop for the excellent manufacturing of the various components. We thank the CERN mechanical workshop for fabricating the nozzles. This research project was supported by the BMBF and the FZ Jülich.

References

1. W. Henkes, Phys. Lett. **12**, 322 (1964); O.F. Hagena, W. Henkes, U. Pfeifer, *Rarefied Gas Dynamics*, Progress in Astronautics and Aeronautics, edited by J. Leith Potter (AIAA, New York, 1976) Vol. 51, p. 1123.
2. E.W. Becker, O.F. Hagena, P.R.W. Henkes, W. Keller, R. Klingelhöfer, B. Krevet, H.O. Moser, Nucl. Eng. Design. **73**, 187 (1982).
3. H.O. Moser, Z. Flugwiss. Weltraumforsch. **11**, 291 (1987).
4. H. Dombrowski, D. Grzonka, W. Hamsink, A. Khoukaz, T. Lister, R. Santo, Nucl. Instr. Meth. A **386**, 228 (1997).
5. A. Khoukaz, T. Lister, C. Quentmeier, R. Santo, C. Thomas, Annual Report 1996/97, Institut für Kernphysik, University Münster.
6. E.W. Becker, H.D. Falter, O.F. Hagena, W. Hences, R. Klingelhöfer, H. Moser, W. Obert, I. Poth, *Proc. Symp. on the Production and Neutralization of Negative Hydrogen Ions and Beams*, Brookhaven, BNL 50 727, 322 (1997).
7. W. Demtröder, H.-J. Föth, Phys. Bl. **43**, 7 (1987).
8. L. Dick, W. Kubischta, *Internal Targets for COSY*, edited by W. Oelert (KFA Jülich, Jül-Spez-409, 1987) III.
9. O. Steinkamp, Ph.D. thesis (KFA Jülich report Jül-2877, 1994); G. Boero, M. LoVetere, M. Macri, S. Passaggio, A. Pozzo, Nuovo Cimento A **109**, 1581 (1996).
10. R. Burgei, M. Garçon, M. Grand, B. Gonel, R. Maillard, A. Malthiery, J. Martin, Nucl. Instr. Meth. **204**, 53 (1982).
11. C. Quentmeier, Diploma thesis, Institut für Kernphysik, University Münster, Germany, 1997.
12. C. Thomas, Diploma thesis, Institut für Kernphysik, University Münster, Germany, 1998.